Electronic Supplementary Material (ESI) for Analyst.

Supporting Information

Conformational analysis of amphetamine and methamphetamine: a comprehensive approach by vibrational and chiroptical spectroscopy

Dobšíková K.[a,†], Michal P.[e,†], Spálovská D.[a], Kuchař M.[b,c,f], Paškanová N.[b,c], Jurok R.[b,c,d], Kapitán J.[e] and Setnička V.[a,*]

[a] Department of Analytical Chemistry, University of Chemistry and Technology, Technická 5, Prague 6, 166 28, Czech Republic

[b] Forensic Laboratory of Biologically Active Substances, University of Chemistry and Technology, Technická 5, Prague 6, 166 28, Czech Republic

[c] Department of Chemistry of Natural Compounds, University of Chemistry and Technology, Technická 5, Prague 6, 166 28, Czech Republic

[d] Department of Organic Chemistry, University of Chemistry and Technology, Technická 5, Prague 6, 166 28, Czech Republic

[e] Department of Optics, Palacký University Olomouc, 17. listopadu 12, Olomouc, 771 46, Czech Republic

[f] National Institute of Mental Health, Topolová 748, Klecany 250 67, Czech Republic

* corresponding author: Vladimir.Setnicka@vscht.cz

† These two authors contributed equally to this work.

Contents

1. The synthesis of amphetamine and methamphetamine hydrochlorides

1-Phenylpropan-2-one oxime

The solution of sodium carbonate (6.36 g, 60 mmol) in water (25 mL) was added in the solution of 1-phenylpropan-2-one (10.00 g, 74.5 mmol) and hydroxylamine hydrochloride (3.22 g, 97.7 mmol) in methanol (60 mL). The mixture was refluxed for 2 h, most of the methanol was evaporated, the rest was extracted with diethyl ether and the ether layer was dried over $MgSO_4$. Evaporation of the solvent gave colorless oil (10.56 g, 95 %), which solidified upon cooling. This crude product was used in next step without further purification. ^{1}H NMR (400 MHz, $CDCl_3$) δ = 8.31 (bs, 1H), 7.33–7.21 (m, 5H), 3.50 (s, 2H), 1.82 (s, 3H).

1-Phenylpropan-2-amine

The 1-phenylpropan-2-one oxime (10.46 g, 70.1 mmol) was dissolved in dry propan-1-ol (170 mL) and the solution was brought to a boil. Heating was stopped and elemental sodium (17.52 g, 0.762 mol) was added at such a rate as to maintain vigorous reflux. At the end, the reaction was slower, so the heating was turned back on to the speed reaction up. The reaction mixture was acidified with concentrated hydrochloric acid (ca 75 mL), cooled, and most of the propanol was evaporated. The residue was diluted with water (200 mL) and extracted with dichloromethane. Sodium hydroxide pellets were then added to the aqueous layer until it was basic, and an oil had separated. The oil was extracted with dichloromethane (2 x 100 mL), dried over K_2CO_3 and the solvent was evaporated. The remaining crude amine was distilled under reduced pressure (bp 77–78 ° C/9 torr) to provide 1-phenylpropan-2-amine 8.45 g (89 %) as a colorless liquid. ^{1}H NMR (400 MHz, $CDCl_3$) δ = 7.36–7.26 (m, 2H), 7.23–7.13 (m, 3H), 3.26–3.10 (m, 1H), 2.72 (dd, *J* = 13.2, 5.4 Hz, 1H), 2.53 (dd, *J* = 13.2, 8.0 Hz, 1H), 1.25 (br s, 2H), 1.13 (d, *J* = 6.3 Hz, 3H).

Racemic 1-phenylpropan-2-amine (8.40 g, 62.1 mmol) and (2*R*,3*R*)-tartaric acid (10.26 g, 68.3 mmol) were dissolved in methanol (200 mL) at reflux. The solution was allowed to cool

to room temperature under occasional stirring to effect crystallization. The crystals were filtered off and recrystallized five times from methanol to afford (*S*)-1-phenylpropan-2-amine·(2*R*,3*R*)-hydrogentartrate (4.51 g, 51 %). Methanol was evaporated from the collected mother liquors, the residue was basified with NaOH, the liberated amine was isolated and treated analogously with (2*S*,3*S*)-tartaric acid to afford (*R*)-1-phenylpropan-2-amine·(2*S*,3*S*)-hydrogentartrate (5.49 g, 62 %). The (*S*)-1-phenylpropan-2-amine·(2*R*,3*R*)-hydrogentartrate (4.51 g, 15.8 mmol) was dissolved in water (20 mL) and basified with solid sodium hydroxide. The oil was extracted with diethyl ether (2 x 30 mL), dried over K_2CO_3, the solvent was evaporated, and the remaining free base dissolved in propan-2-ol (5 mL). The solution was treated with hydrogen chloride in ether (2 M) to make the pH slightly acidic and then was allowed to crystallize overnight in a refrigerator. The formed crystals were filtered off with suction, washed with diethyl ether and dried in vacuum to provide (*S*)-1-phenylpropan-2-amine hydrochloride (2.17 g), mp 153154 °C, $[\alpha]_D = 24.2°$ (H_2O, c = 5). From (*R*)-1-phenylpropan-2-amine·(2*S*,3*S*)-hydrogentartrate (5.49 g, 19.2 mmol) was analogously obtained (*R*)-1-phenylpropan-2-amine hydrochloride (2.65 g), mp 154–155 °C, $[\alpha]_D = –24.7°$ (H_2O, c = 5.00).

(*R*)-*N*-Methyl-1-phenylpropan-2-amine

Methyl chloroformate (0.60 g, 6.3 mmol) was added to the ice cooled solution of (*R*)-1-phenylpropan-2-amine hydrochloride (1.00 g, 5.8 mmol) in dichloromethane (35 mL), then the solution of NaOH (0.47 g, 11.8 mmol) in water (10 mL) was added dropwise with stirring. The mixture was stirred at room temperature for 3 h; the organic layer was separated, washed with water (15 mL), dried with $MgSO_4$ and evaporated to provide appropriate carbamate (1.11 g, 99 %). The solution of the carbamate in dry THF (10 mL) was added dropwise to the ice cooled stirred solution of LAH (0.66 g, 17.4 mmol) in dry THF (20 mL) under argon atmosphere and then the mixture was refluxed for 2 h. The mixture was cooled in ice bath and in order: water (0.6 mL), 15% NaOH solution (0.6 mL) and again water (1.8 mL) was added under stirring. The white precipitate was filtered and washed several times with THF. The combined tetrahydrofuran solution was dried with $MgSO_4$, filtered, and evaporated to leave a crude free base of (*R*)-*N*-methyl-1-phenylpropan-2-amine (0.85 g, 99 %). The free base was dissolved in diethyl ether and converted to the hydrochloride salt by the addition of a solution of HCl in diethyl ether. The precipitate was filtered off with suction and crystallized from acetonitrile to afford (*R*)-*N*-methyl-1-phenylpropan-2-amine hydrochloride (0.90 g, 85 %) as white needles, mp 174–175 °C, $[\alpha]_D = –24.9°$ (H_2O, c = 4.00). ^{1}H NMR (400 MHz, $CDCl_3$): δ = 9.73(bs, 2H),

7.32−7.21 (m, 5H), 3.49 (dd, *J* = 13.0, 4.1 Hz, 1H), 3.35 (m, 1H), 2.85(dd, *J* = 13.0, 9.9 Hz, 1H), 2.70 (s, 3H), 1.35 (d, *J*= 6.5 Hz, 3H). ^{13}C NMR ($CDCl_3$, 100 MHz): δ = 135.9, 129.1, 128.6, 127.0, 56.9, 39.1, 30.0, 15.2. C10H15N·HCl, (M+)/z: 149.24, Found: (M +H)/z: 150.0

2. The preparative enantioseparation method

An Acquity UltraPerformance Convergence Chromatography TM (UPC2) from Waters (Milford, MA, USA) was used. The system featured a binary solvent delivery pump, an autosampler, an automated back-pressure regulator, a column oven compatible with 250 mm long columns (Lux Amylose-2, 250 × 4.6 mm, 5 μm) and a photodiode array (PDA) detector. The column Chiral ART Amylose-C (250 × 4.6 mm, S-5 μm) from YMC Europe GmbH (Dinslaken, Germany) was used. As mobile phase was used carbon dioxide with propan-2-ol (iPrOH) + 0.1 % isopropylamine (IPA). An isocratic solvent manager was used to deliver a make-up solvent (MeOH/H_2O/FA, 90/10/0.1, v/v/v) to the column effluent prior a mass detector. The flow rate of make-up solvent was 0.3 mL min^{-1}. The mass detector was a single quadrupole (QDa, Waters, Milford, MA, USA) with electrospray ionization. The parameters were as follow: probe temperature 300 °C, source temperature 120 °C, nitrogen flow rate 5 L min^{-1}, capillary voltage 0.8 kV, cone voltage 9 V. The analytes were detected in positive ionization mode (100–400 Da) at their exact molecular mass (actually $[M + H]^+$). The chromatographic system was controlled by Empower® 3 software (Waters, Milford, MA, USA).

The chromatographic measurements were performed at a flow rate 2.5 mL min^{-1}, the column temperature was 35 °C, back pressure was 2001 psi (138 bar). The ratio of mobile phase for enantioseparation of methamphetamine was set to 95/5 (CO_2/iPrOH + 0.1 % IPA, v/v) and for amphetamine was set to 97.5/2.5 (CO_2/iPrOH + 0.1 % IPA, v/v). The stock solutions of analytes were prepared in MeOH at a concentration of 1 mg mL^{-1} store at 5 °C. A solution of analytes at a concentration of 100 μg mL^{-1} were used for analyses. The void volume was determined using the solvent peak. The injection volume was 2 μL and the autosampler temperature was set to 10 °C. All measurements were performed in triplicate.

The (*S*)-enantiomer of methamphetamine hydrochloride were eluted as the first detected peak followed by the (*R*)-enantiomer. The representative chromatograms are below (Fig. S1).

The purity of the enantiomers was determined from ratio of peaks area. Purity of (*S*)-methamphetamine hydrochloride was 100 % and for (*R*)-enantiomer was 99.63 % (Table S1).

In the case of amphetamine hydrochloride, the (*R*)-enantiomer were eluted as the first detected peak followed by the (*S*)-enantiomer. The representative chromatograms follow below (Fig. S2). The purity of the enantiomers was determined as a ratio of the peak areas. The purity of (*R*)-amphetamine hydrochloride was 98.72 % and for (*S*)-amphetamine it was 99.72 % (Table S2).

Table S1 The retention time (R_t), selectivity (α), resolution (R_s) and area stated for the enantioseparation of amphetamine hydrochloride.

(*R*)-amphetamine hydrochloride					**(*S*)-amphetamine hydrochloride**				
Enantiomer	R_t [min]	α	R_s	Area [%]	Enantiomer	R_t [min]	α	R_s	Area [%]
(*S*)-	21.85	1.28	3.52	98.72	(*S*)-	21.86	1.28	3.36	0.28
(*R*)-	27.81			1.28	(*R*)-	27.77			99.72

Table S2 The retention time (R_t), selectivity (α), resolution (R_s) and area stated for the enantioseparation of methamphetamine hydrochloride.

(*S*)-methamphetamine hydrochloride					**(*R*)-methamphetamine hydrochloride**				
Enantiomer	R_t [min]	α	R_s	Area [%]	Enantiomer	R_t [min]	α	R_s	Area [%]
(*S*)-	8.60	-	-	100.00	(*S*)-	8.65	1.13	1.64	0.37
(*R*)-	-			-	(*R*)-	9.66			99.63

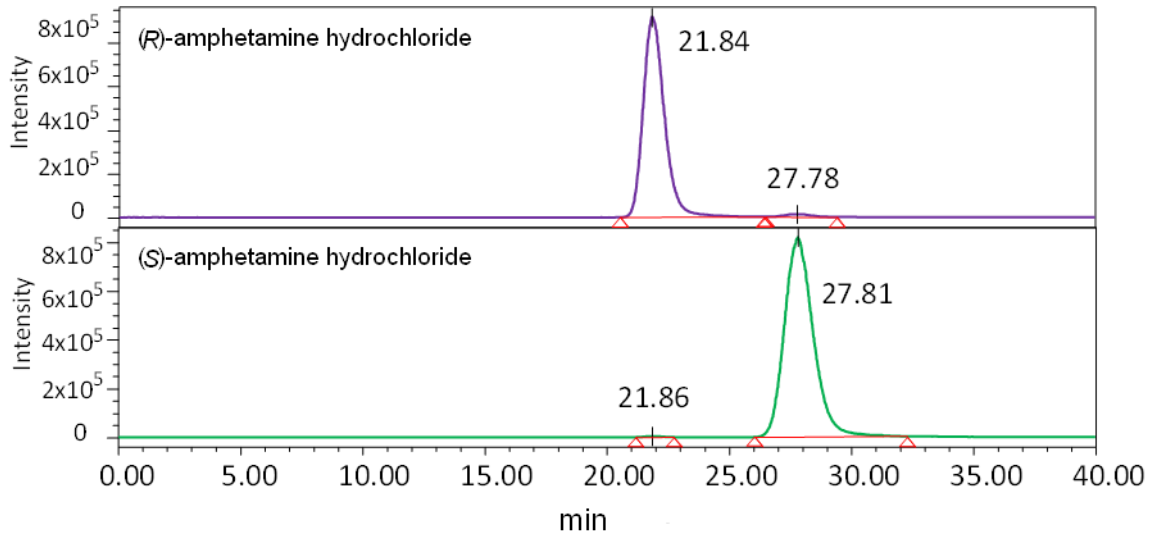

Fig. S1 Chromatogram of (*R*)-amphetamine is above (purple) and the (*S*)-amphetamine hydrochloride below (green).

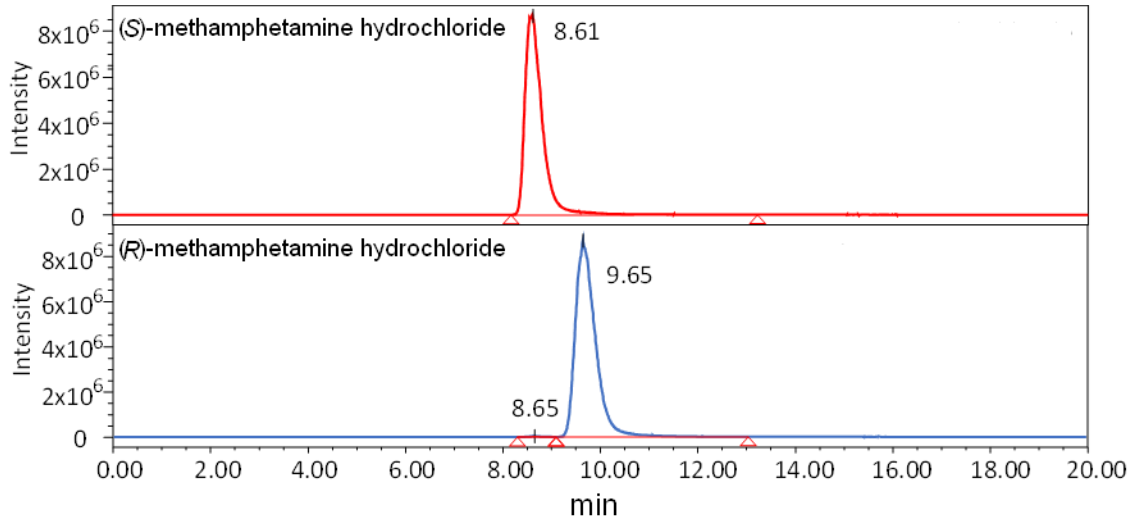

Fig. S2 Chromatogram of (*S*)-methamphetamine is above (red) and (*R*)-methamphetamine hydrochloride is below (blue).

3. VCD and ROA spectroscopy

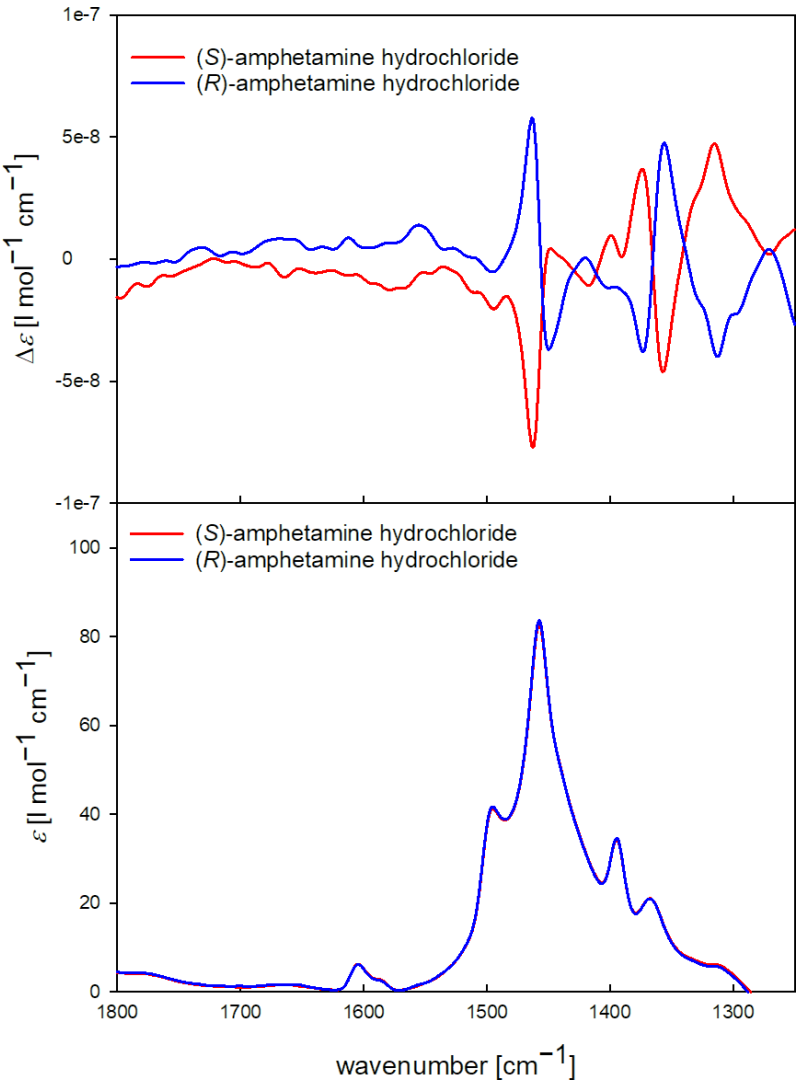

Fig. S3 Experimental VCD (top) and IR absorption spectra (bottom) of both amphetamine hydrochloride enantiomers; the intensity is in epsilon units (L mol^{-1} cm^{-1}).

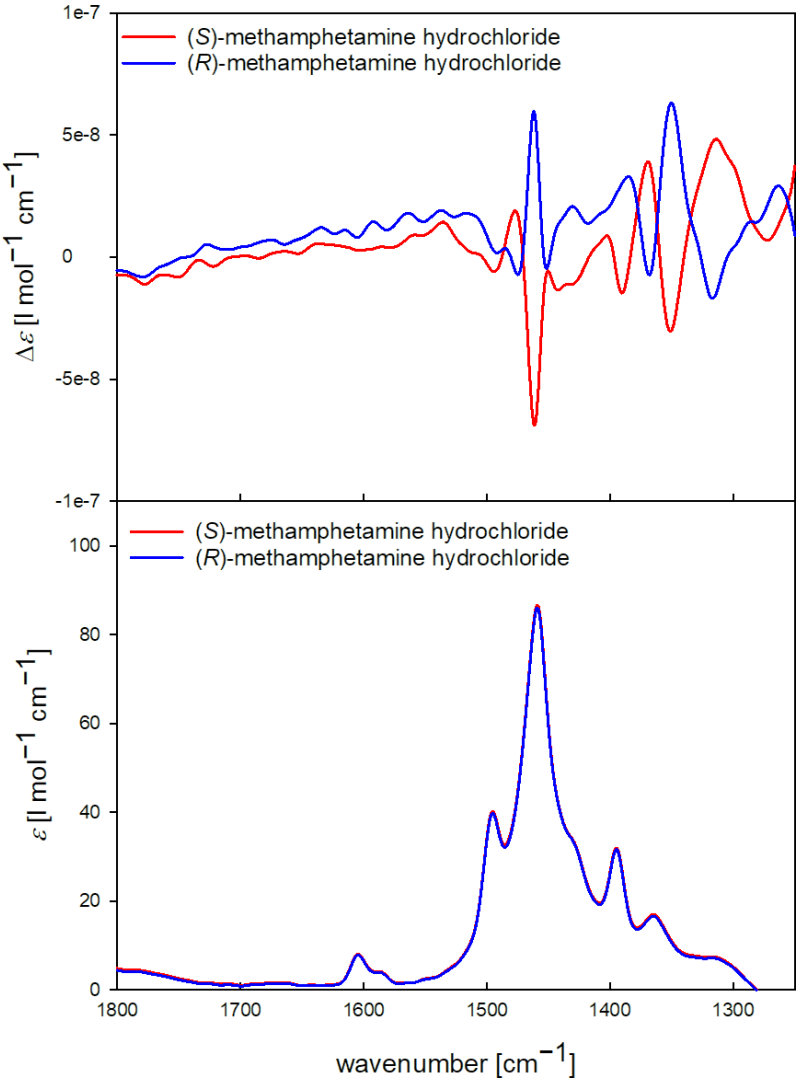

Fig. S4 Experimental VCD (top) and IR absorption spectra (bottom) of both methamphetamine hydrochloride enantiomers; the intensity is in epsilon units (L mol^{-1} cm^{-1}).

Table S3 Experimental conditions of the Raman and ROA measurement.

sample name	sample weight [g]	solvent name	solvent volume [uL]	exposition time [h]	laser power at sample [mW]
(*R*)-amphetamine hydrochloride	0.01	water	90	12.9	402
(*S*)-amphetamine hydrochloride	0.01	water	90	9.4	618
(*R*)-methamphetamine hydrochloride	0.01	water	90	9.9	642
(*S*)-methamphetamine hydrochloride	0.01	water	90	9.2	642

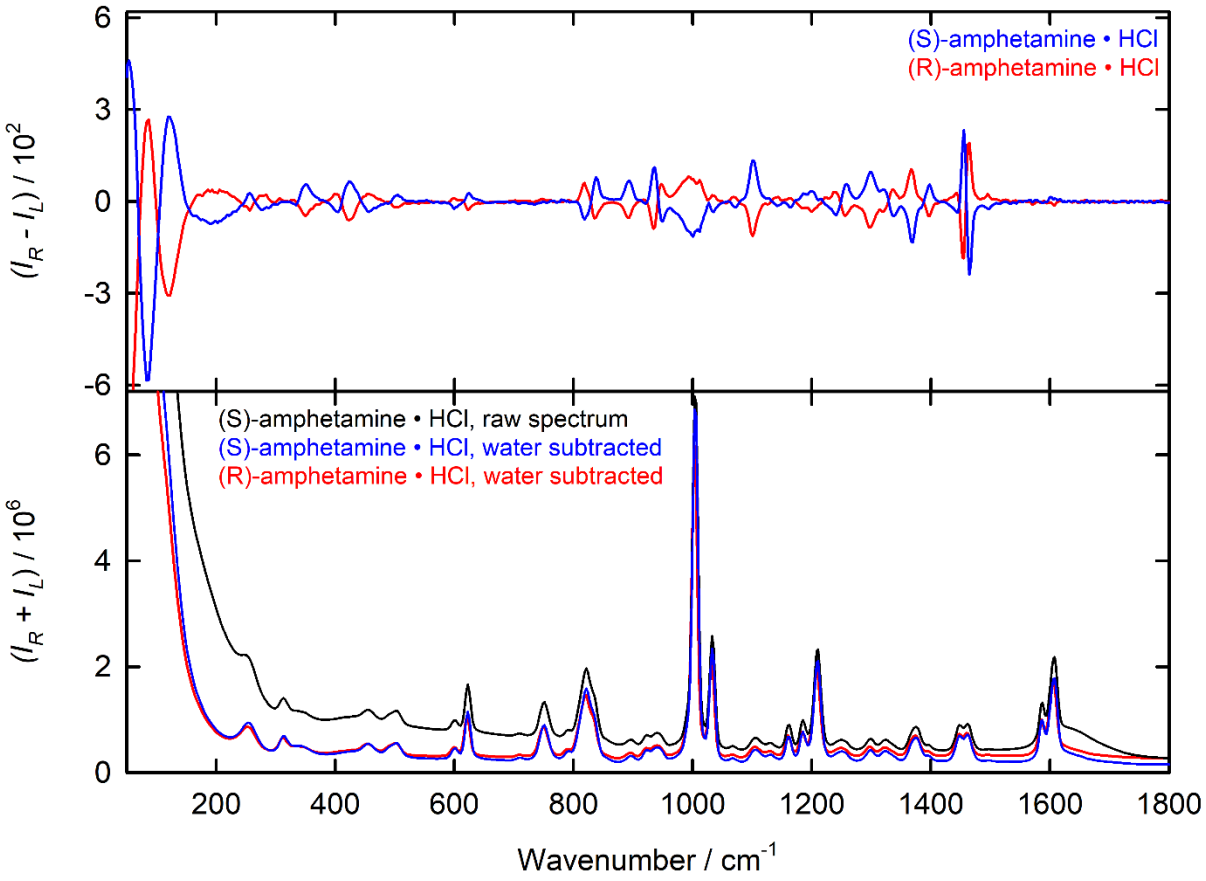

Fig. S5 Experimental ROA ($I_R - I_L$) and Raman ($I_R + I_L$) spectra of both amphetamine hydrochloride enantiomers; the intensity is in (e^- cm J^{-1}).

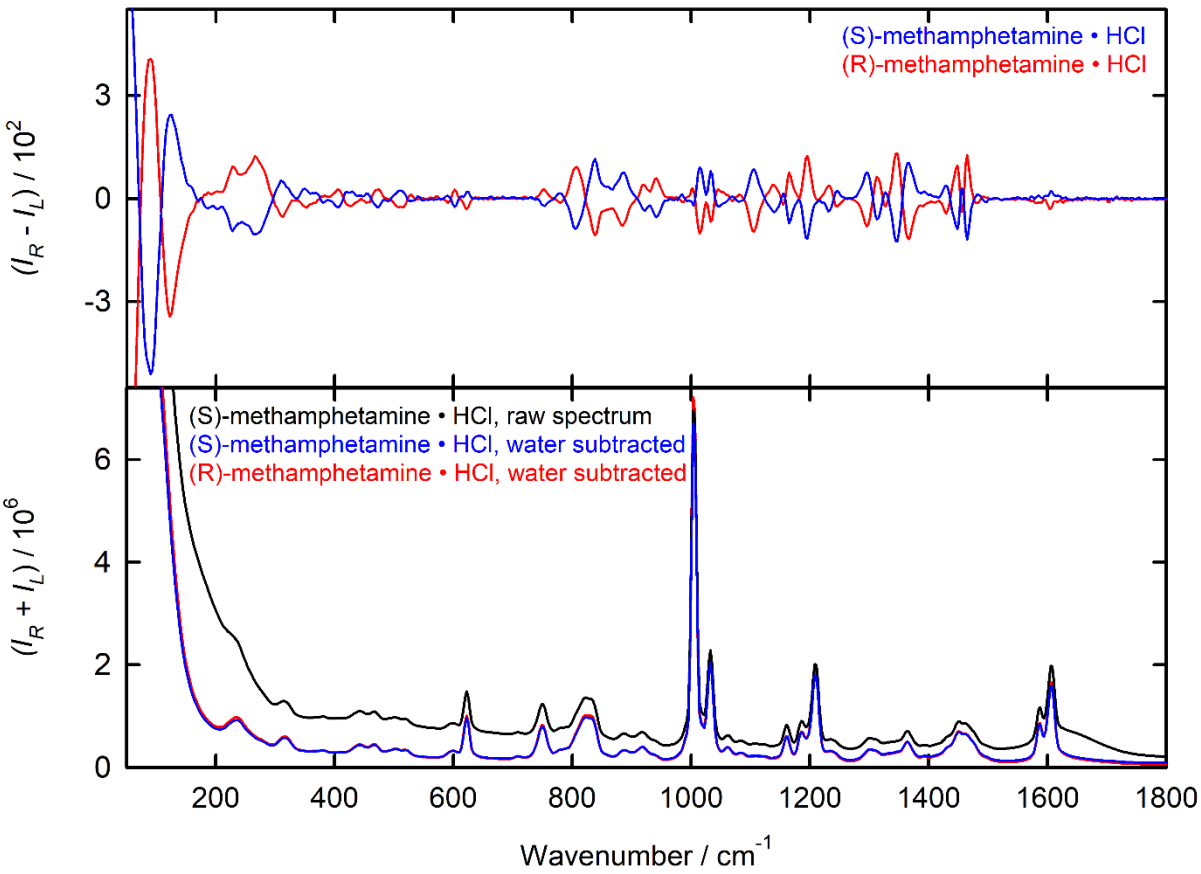

Fig. S6 Experimental ROA ($I_R - I_L$) and Raman ($I_R + I_L$) spectra of both methamphetamine hydrochloride enantiomers; the intensity is in (e^- cm J^{-1}).

4. Single molecule and MD calculations

Calculated Raman and ROA intensities

It can be shown that Raman and ROA intensities of the vibrational transition *k* in a harmonic approximation are proportional to the respective cross-sections for this transition:

$$\frac{\partial\sigma_k}{\partial\Omega} = \frac{\mu_0^2 c^3 h}{8}\frac{\tilde{\nu}^4}{\tilde{\nu}_k}\left\langle\left(\frac{\partial\alpha_{\alpha\beta}}{\partial Q_k}\right)^2,\left(\frac{\partial G'_{\alpha\beta}}{\partial Q_k}\right)^2,\ldots\right\rangle B(\tilde{\nu}_k,T) \tag{S1}$$

where $\tilde{\nu}_0$ is the wavenumber of incident radiation, $\tilde{\nu}_k$ is the wavenumber of scattered radiation, $\tilde{\nu} = \tilde{\nu}_0 - \tilde{\nu}_k$ and Boltzmann factor $B(\tilde{\nu}_k,T) = \left(1-\exp\left(-\frac{hc\tilde{\nu}_k}{kT}\right)\right)^{-1}$ originating from summing over allowed transitions between the state populated at thermal equilibrium. Brackets signify tensor invariant combinations depending on experimental arrangement. For example, the combination of tensor invariants in brackets is $\alpha^2 + {}^{7}\!/_{45}\beta(\alpha)^2$ for unpolarized (total) backscattering and SCP modulation. This equation supposes that both excitation and scattered radiant fluxes are counted in watts. In contrast, all modern detectors work in photon counting regime where number of photons per detection time is recorded instead. For the simulated spectra we therefore used a slightly modified version of Raman scattering cross-sections reflecting this situation as:

$$\frac{\partial\sigma_k}{\partial\Omega} = \frac{\mu_0^2 c^2}{8}\frac{\tilde{\nu}^3}{\tilde{\nu}_k}\left\langle\left(\frac{\partial\alpha_{\alpha\beta}}{\partial Q_k}\right)^2,\left(\frac{\partial G'_{\alpha\beta}}{\partial Q_k}\right)^2,\ldots\right\rangle B(\tilde{\nu}_k,T) \tag{S2}$$

Finally, the spectral scattering cross-section (a "spectrum") was generated from the calculated scattering cross-sections for Lorentzian line-shapes as:

$$\beta_{\tilde{\nu}}(\tilde{\nu}) = \sum_{k=1}^{3N-6}\frac{2}{\pi\sigma}\frac{1}{4\left(\frac{\tilde{\nu}-\tilde{\nu}_k}{\sigma}\right)^2+1}\frac{\partial\sigma_k}{\partial\Omega} \tag{S3}$$

where *N* is the number of vibrational modes and σ is the full width at half maximum (FWHM) of the peaks.

Table S4 Stable conformers of amphetamine and methamphetamine with their characteristic torsional angles, relative Gibbs free energies and Boltzmann weights simulated at the B3PW91/6-311++G** level.

Conformer	Torsional angle (°)			Δ*G* (kcal/mol)	Boltzmann weights
	α_1	α_2	α_3		
Amphetamine I	72	58	−	0	0.78
Amphetamine II	−76	172	−	0.95	0.16
Amphetamine III	96	−63	−	1.44	0.07
Methamphetamine I	72	58	−167	0	0.77
Methamphetamine II	107	171	−172	1.10	0.12
Methamphetamine III	96	−64	−177	1.83	0.03
Methamphetamine IV	65	67	−82	2.30	0.02
Methamphetamine V	−76	167	63	1.99	0.03
Methamphetamine VI	92	−60	−75	1.85	0.03

Table S5 Conformer categories of amphetamine and methamphetamine with their normalized population obtained during the free molecular dynamics run (100 ns, 10000 snapshots).

Conformer	Torsional angle (°)		Normalized MD population
	α_2	α_3	
Amphetamine I	0 – 120°	−	0.50
Amphetamine II	120 – 240°	−	0.10
Amphetamine III	240 – 360°	−	0.39
Methamphetamine I	0 – 120°	120 – 240°	0.22
Methamphetamine II	120 – 240°	120 – 240°	0.37
Methamphetamine III	240 – 360°	120 – 240°	0.32
Methamphetamine IV	0 – 120°	240 – 360°	0.03
Methamphetamine V	120 – 240°	240 – 360°	0.03
Methamphetamine VI	240 – 360°	240 – 360°	0.03

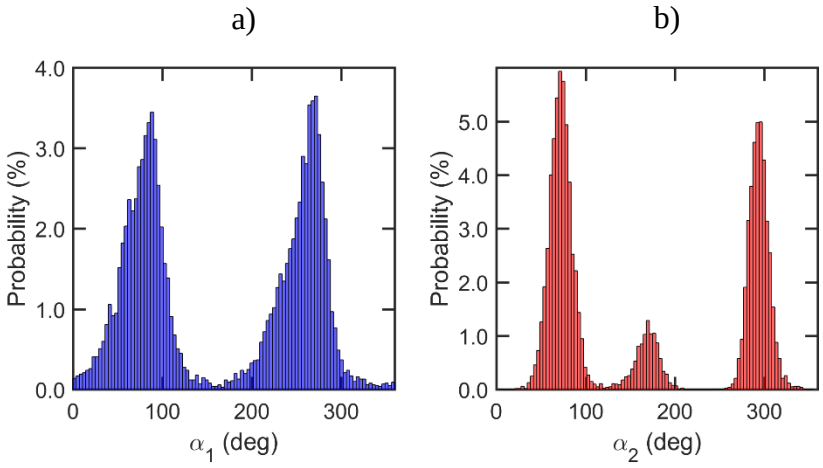

Fig. S7 Distributions of the amphetamine characteristic angles obtained during the free molecular dynamics run (100 ns, 10000 snapshots).

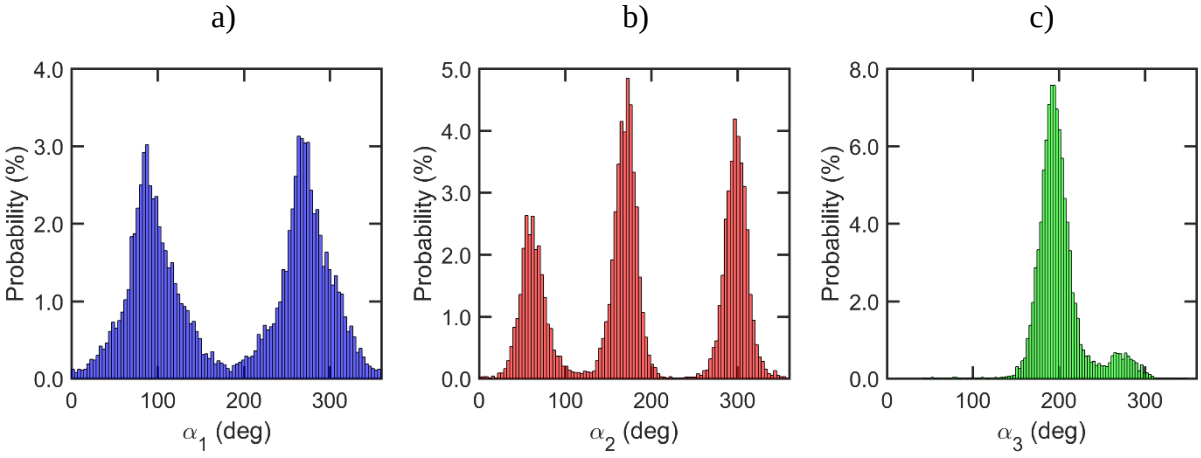

Fig. S8 Distributions of the methamphetamine characteristic angles obtained during the free molecular dynamics run (100 ns, 10000 snapshots).

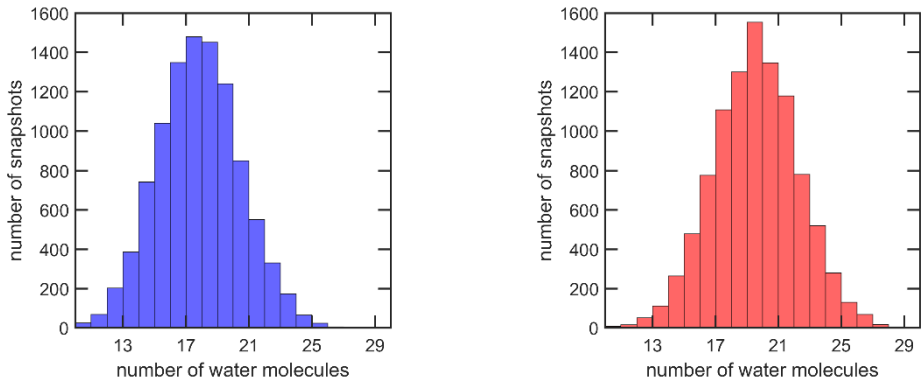

Fig. S9 MD distribution of the water molecules in the first solvation shell defined by distance 3 Å of water from amphetamine (blue) and methamphetamine (red) molecules used for DFT calculations of clusters.

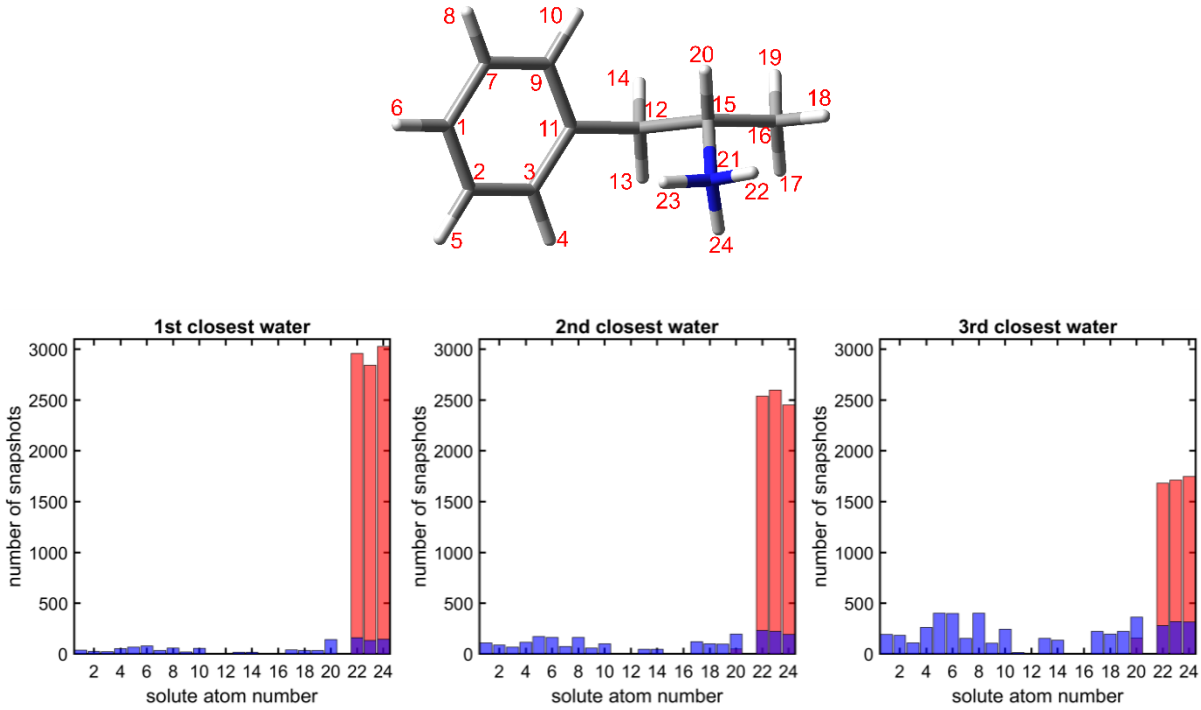

Fig. S10 MD distribution of three closest water molecules to the amphetamine (100 ns MD, 10000 snapshots). Blue bars mark interaction with H-atom, while the red bars with O-atom of H_2O molecule.

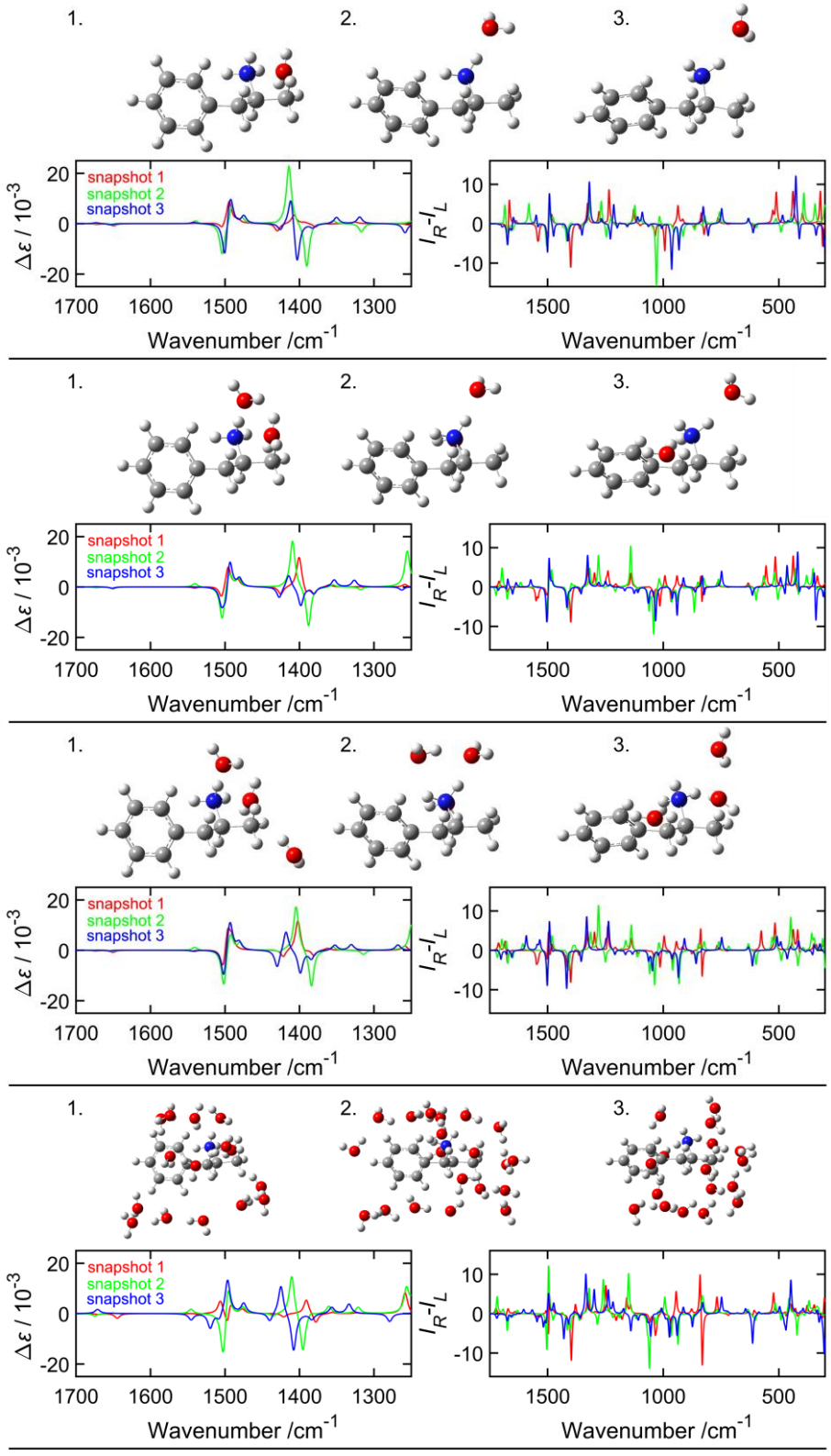

Fig. S11 Comparison of calculated VCD (left) and ROA (right) spectra of (*S*)-amphetamine hydrochloride conformer **I** with one, two, three closest water molecules and the cluster with the whole first solvation shell. Spectra of the three representatives (snapshot 1 – 3) of conformer **I** are overlaid in each figure.

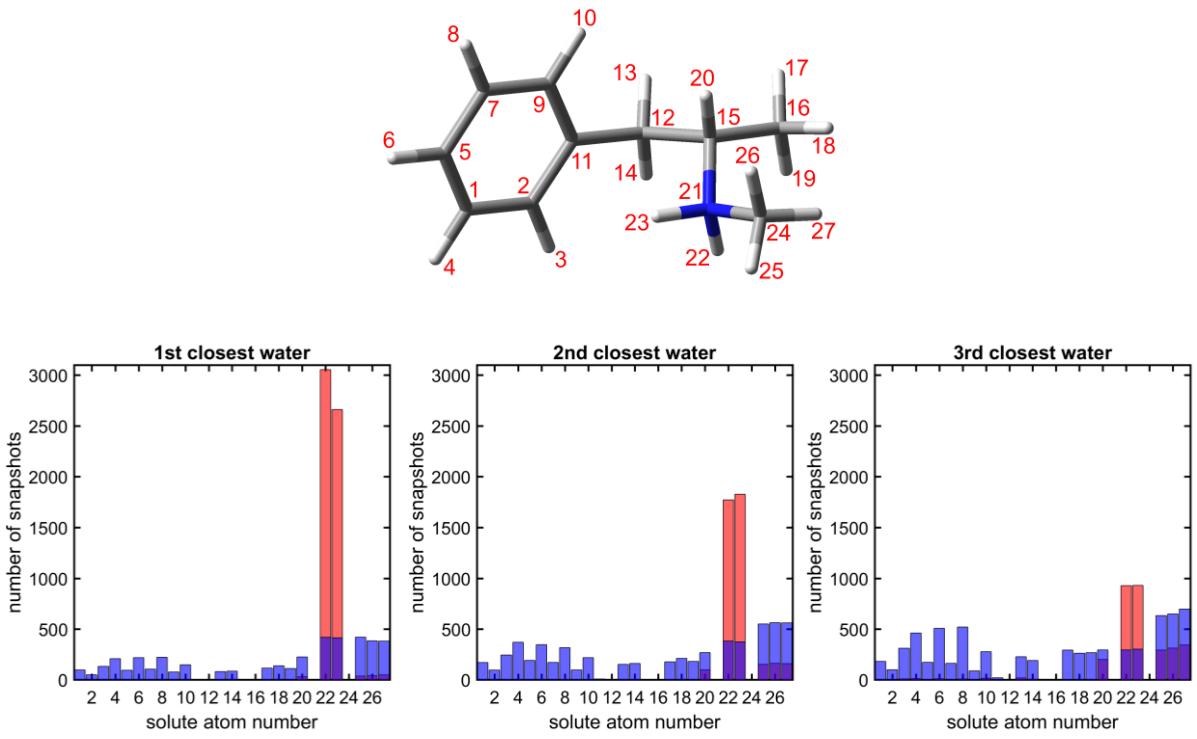

Fig. S12 MD distribution of three closest water molecules to the methamphetamine (100 ns MD, 10000 snapshots). Blue bars mark interaction with H-atom, while the red bars with O-atom of H_2O molecule.

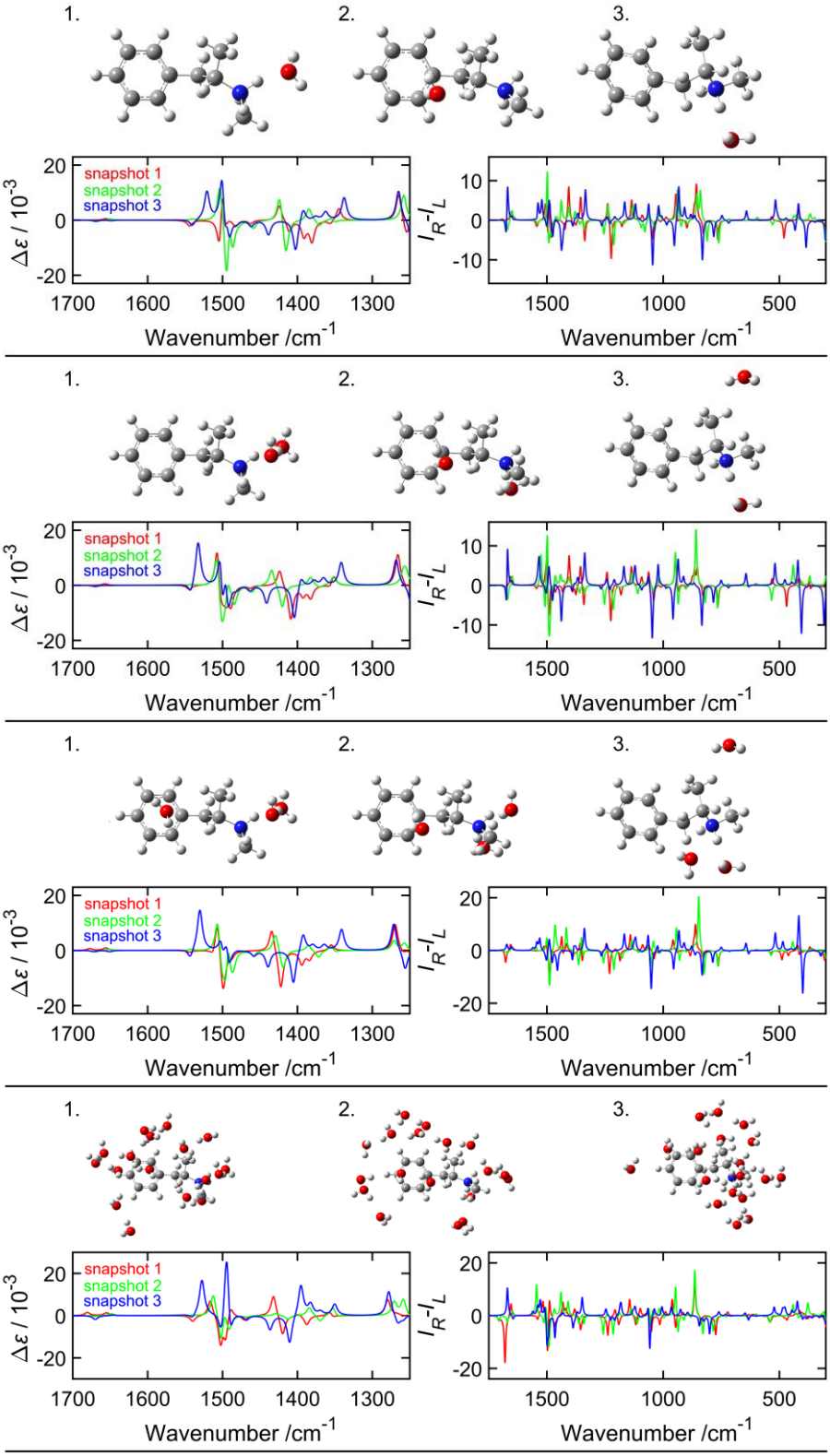

Fig. S13 Comparison of calculated VCD (left) and ROA (right) spectra of (*S*)-methamphetamine hydrochloride conformer **I** with one, two, three closest water molecules and the cluster with the whole first solvation shell. Spectra of the three representatives (snapshot 1 – 3) of conformer **I** are overlaid in each figure.

Table S6 Similarity factors and wavenumber scaling factors (S.f.) of three amphetamine conformers calculated at several levels of DFT theory (single molecule calculations with COSMO) and compared to the experimental spectrum separately in the spectral range of 1700–1250 cm^{-1} for IR and VCD spectra, 1550–1300 cm^{-1} for DF spectra, 1750–300 cm^{-1} for Raman, ROA, and CID spectra.

DFT	**IR**				**VCD**				**DF**			
Level	**S.f.**	**I**	**II**	**III**	**S.f.**	**I**	**II**	**III**	**S.f.**	**I**	**II**	**III**
1	0.98	0.76	0.72	0.68	0.98	0.40	0.34	-0.38	0.98	-0.49	0.56	0.48
2	0.98	0.74	0.68	0.69	0.98	0.41	0.36	-0.34	0.98	0.30	0.67	0.51
3	0.99	0.65	0.62	0.66	0.99	0.49	0.33	-0.34	0.99	0.47	0.34	0.50
4	0.98	0.71	0.65	0.66	0.98	0.40	0.31	-0.33	0.98	-0.23	0.55	0.49
5	0.97	0.72	0.64	0.65	0.97	0.33	0.45	-0.32	0.97	-0.54	0.44	0.43
6	0.98	0.64	0.61	0.62	0.98	0.35	0.29	-0.23	0.98	-0.24	0.52	0.20
7	0.97	0.70	0.63	0.65	0.97	0.38	0.42	-0.27	0.97	-0.53	-0.48	0.21
DFT	**Raman**				**ROA**				**CID**			
level	**S.f.**	**I**	**II**	**III**	**S.f.**	**I**	**II**	**III**	**S.f.**	**I**	**II**	**III**
1	0.99	0.74	0.76	0.69	0.98	0.20	-0.15	0.11	0.98	0.21	-0.07	0.15
2	0.99	0.65	0.65	0.62	0.98	0.31	-0.06	0.11	0.98	0.26	-0.08	0.12
3	0.99	0.61	0.58	0.56	0.99	0.28	-0.08	0.16	0.99	0.30	-0.08	0.11
4	0.99	0.69	0.70	0.64	0.98	0.31	-0.06	0.11	0.98	0.29	-0.07	0.13
5	0.98	0.72	0.72	0.67	0.97	0.25	-0.08	0.18	0.97	0.25	-0.08	0.16
6	0.98	0.67	0.66	0.63	0.98	0.16	-0.06	0.16	0.98	0.22	-0.08	0.17
7	0.97	0.75	0.75	0.69	0.97	0.23	-0.09	0.20	0.97	0.26	-0.07	0.20

1 – B3LYP/6-311++G**

2 – B3PW91/6-311++G**

3 – B3PW91/aug-cc-pVDZ

4 – B3PW91/aug-cc-pVTZ

5 – CAM-B3LYP/6-311++G**

6 – CAM-B3LYP/aug-cc-pVDZ

7 – CAM-B3LYP/aug-cc-pVTZ

Table S7 Linear combination coefficients of three stable conformers and similarity factor of amphetamine calculated at several levels of theory (single molecule calculations with COSMO) in the spectral range of 1700–1250 cm^{-1} for IR and VCD spectra, 1550–1300 cm^{-1} for DF spectra.

	level of DFT theory	Linear combination coefficients			Similarity factor	Scaling Factor
		I	II	III		
			IR			
1	**B3LYP/6-311++G****	0.74	0.18	0.08	0.77	0.98
2	**B3PW91/6-311++G****	0.70	0.09	0.20	0.75	0.98
3	**B3PW91/aug-cc-pVDZ**	0.54	0.00	0.46	0.70	0.99
4	**B3PW91/aug-cc-pVTZ**	0.68	0.17	0.16	0.72	0.98
5	**CAM-B3LYP/6-311++G****	0.75	0.14	0.11	0.72	0.97
6	**CAM-B3LYP/aug-cc-pVDZ**	0.43	0.28	0.29	0.66	0.98
7	**CAM-B3LYP/aug-cc-pVTZ**	0.67	0.23	0.10	0.71	0.97
			VCD			
1	**B3LYP/6-311++G****	0.35	0.51	0.14	0.53	0.98
2	**B3PW91/6-311++G****	0.36	0.60	0.04	0.50	0.98
3	**B3PW91/aug-cc-pVDZ**	0.67	0.33	0.00	0.51	0.99
4	**B3PW91/aug-cc-pVTZ**	0.38	0.53	0.09	0.49	0.98
5	**CAM-B3LYP/6-311++G****	0.21	0.73	0.05	0.52	0.97
6	**CAM-B3LYP/aug-cc-pVDZ**	0.55	0.45	0.00	0.42	0.98
7	**CAM-B3LYP/aug-cc-pVTZ**	0.32	0.62	0.06	0.52	0.97
			DF			
1	**B3LYP/6-311++G****	0.26	0.57	0.17	0.71	0.97
2	**B3PW91/6-311++G****	0.24	0.55	0.22	0.77	0.98
3	**B3PW91/aug-cc-pVDZ**	0.30	0.40	0.29	0.76	0.98
4	**B3PW91/aug-cc-pVTZ**	0.18	0.50	0.31	0.76	0.98
5	**CAM-B3LYP/6-311++G****	0.30	0.39	0.31	0.68	0.97
6	**CAM-B3LYP/aug-cc-pVDZ**	0.19	0.45	0.36	0.59	0.98
7	**CAM-B3LYP/aug-cc-pVTZ**	0.30	0.35	0.35	0.58	0.97

Table S8 Linear combination coefficients of three stable conformers and similarity factor of amphetamine Raman, ROA and CID spectra calculated at several levels of theory in the spectral range of 1750–300 cm^{-1}.

	level of DFT theory	Linear combination coefficients			Similarity Factor	Scaling Factor
		I	II	III		
			Raman			
1	**B3LYP/6-311++G****	0.21	0.60	0.19	0.78	0.99
2	**B3PW91/6-311++G****	0.35	0.41	0.24	0.68	0.99
3	**B3PW91/aug-cc-pVDZ**	0.30	0.31	0.39	0.40	0.96
4	**B3PW91/aug-cc-pVTZ**	0.31	0.45	0.24	0.72	0.99
5	**CAM-B3LYP/6-311++G****	0.31	0.45	0.24	0.75	0.98
6	**CAM-B3LYP/aug-cc-pVDZ**	0.38	0.33	0.29	0.70	0.98
7	**CAM-B3LYP/aug-cc-pVTZ**	0.30	0.45	0.25	0.78	0.97
			ROA			
1	**B3LYP/6-311++G****	0.73	0.00	0.27	0.22	0.98
2	**B3PW91/6-311++G****	0.60	0.13	0.26	0.34	0.98
3	**B3PW91/aug-cc-pVDZ**	0.55	0.07	0.38	0.33	0.99
4	**B3PW91/aug-cc-pVTZ**	0.63	0.09	0.28	0.32	0.98
5	**CAM-B3LYP/6-311++G****	0.50	0.06	0.44	0.30	0.97
6	**CAM-B3LYP/aug-cc-pVDZ**	0.40	0.11	0.49	0.22	0.98
7	**CAM-B3LYP/aug-cc-pVTZ**	0.46	0.02	0.52	0.29	0.97
			CID			
1	**B3LYP/6-311++G****	0.57	0.17	0.26	0.27	0.98
2	**B3PW91/6-311++G****	0.59	0.25	0.16	0.34	0.98
3	**B3PW91/aug-cc-pVDZ**	0.57	0.24	0.18	0.37	0.99
4	**B3PW91/aug-cc-pVTZ**	0.58	0.27	0.15	0.38	0.98
5	**CAM-B3LYP/6-311++G****	0.55	0.18	0.27	0.34	0.97
6	**CAM-B3LYP/aug-cc-pVDZ**	0.50	0.18	0.32	0.33	0.98
7	**CAM-B3LYP/aug-cc-pVTZ**	0.47	0.14	0.39	0.36	0.97

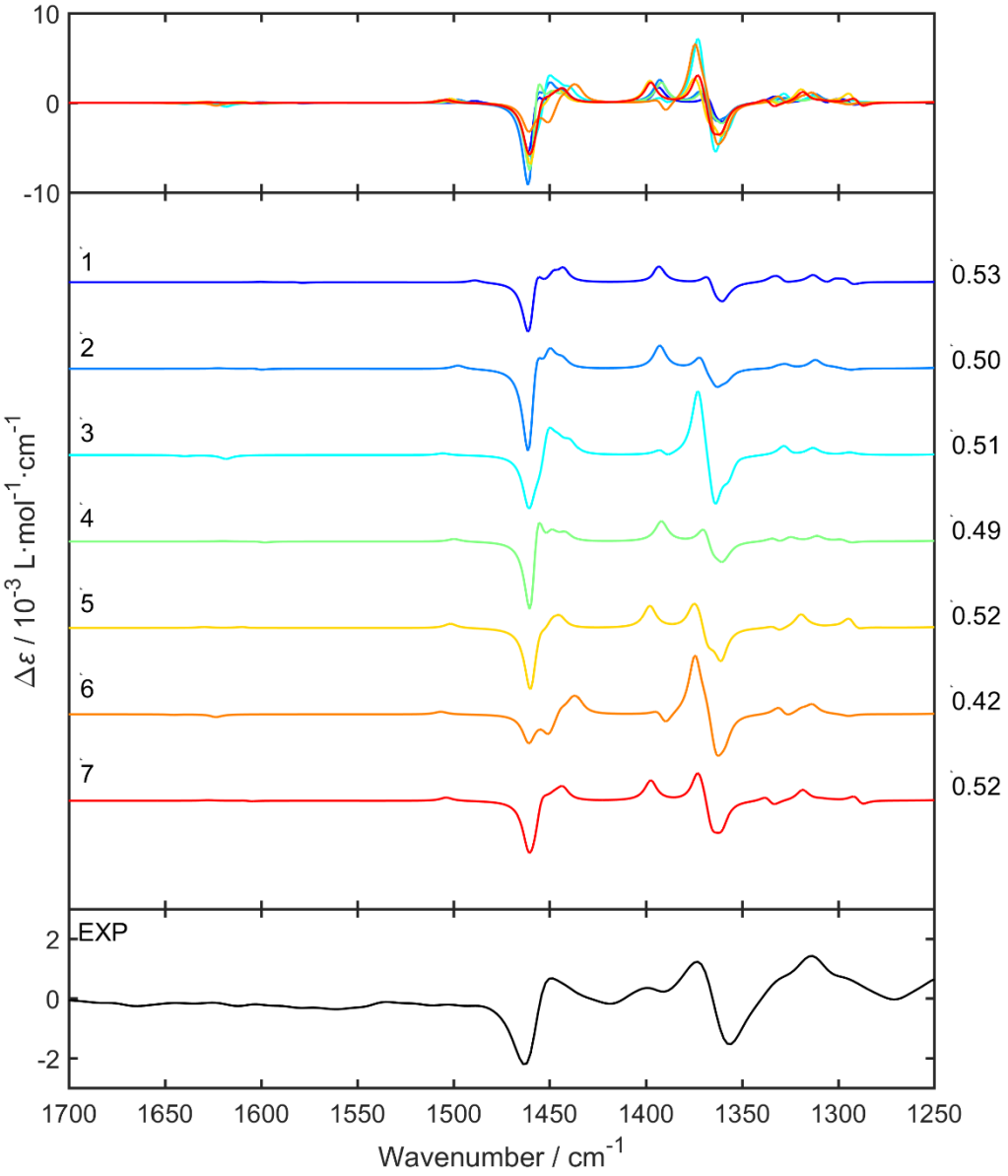

Fig. S14 Comparison of experimental and calculated VCD spectrum of (*S*)-amphetamine hydrochloride according to **Table S7**. The overall similarity for the conformational mixture is marked on the right. The overlaid VCD spectra 1–7 are on the top.

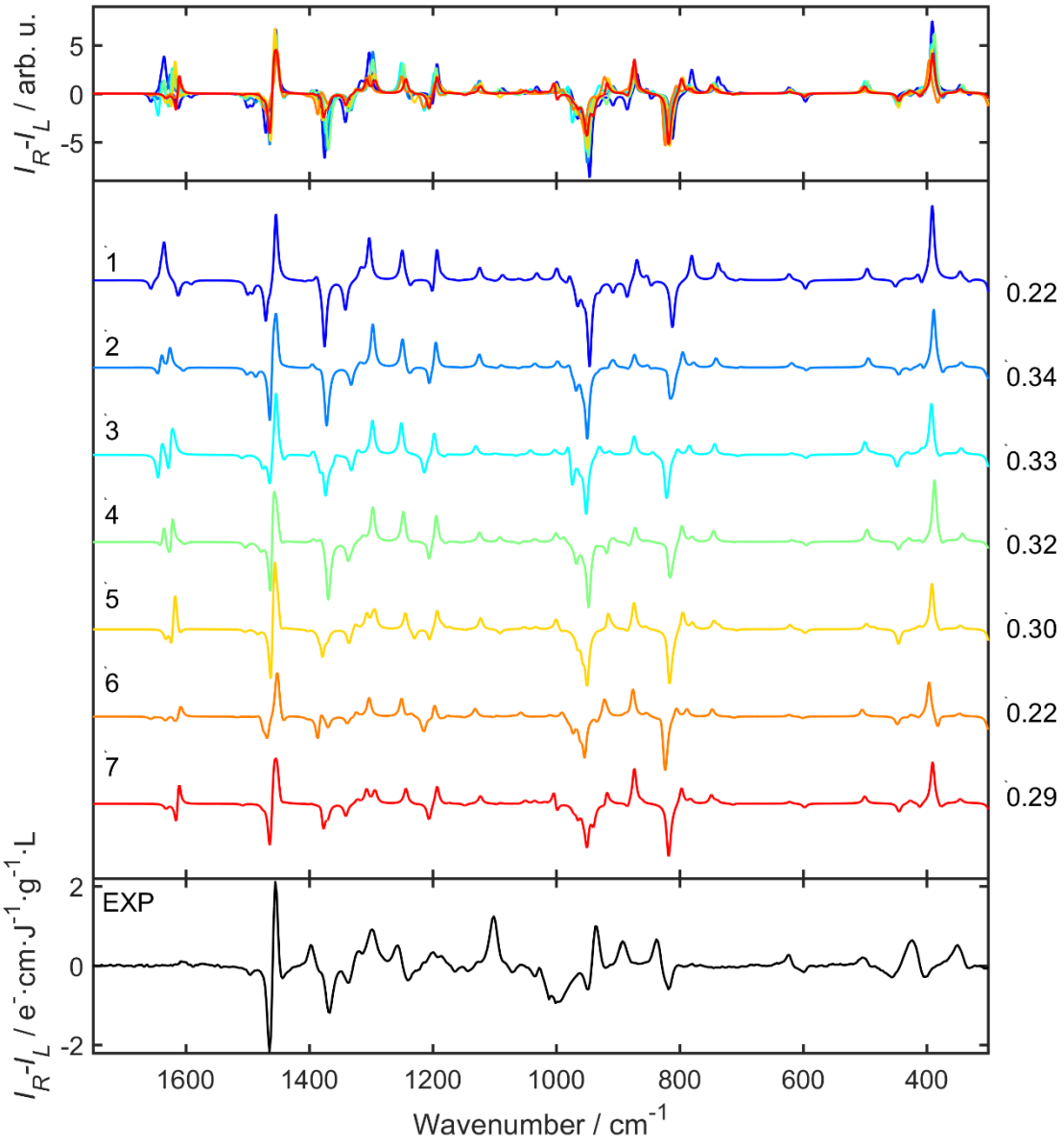

Fig. S15 Comparison of experimental and calculated ROA spectrum of (*S*)-amphetamine hydrochloride according to **Table S8**. The overall similarity in percentage for the conformational mixture is marked on the right. The overlaid ROA spectra 1–7 are on the top.

Table S9 Comparison of ROA similarity factors for linear combination of three and six conformers of amphetamine and methamphetamine, respectively, calculated for different spectral ranges at the B3PW91/6-311++G** level (single molecule geometries).

amphetamine							
Label	**Wavenumber Range**		**Linear combination coefficients**			**Similarity Factor**	**Scaling Factor**
			I	**II**	**III**		
1	300	1750	0.60	0.13	0.26	0.34	0.98
2	300	1550	0.59	0.15	0.26	0.34	0.98
3	700	1550	0.61	0.23	0.16	0.41	0.98
4	1000	1550	0.61	0.39	0.00	0.59	0.98
5	1400	1550	0.54	0.46	0.00	0.96	0.98
6	50	300	0.45	0.27	0.28	0.64	1.00

methamphetamine										
Label	**Wavenumber Range**		**Linear combination coefficients**						**Similarity factor**	**Scaling Factor**
			I	**II**	**III**	**IV**	**V**	**VI**		
1	300	1750	0.21	0.16	0.07	0.11	0.36	0.08	0.41	0.98
2	300	1550	0.24	0.16	0.09	0.08	0.35	0.08	0.42	0.98
3	700	1550	0.22	0.09	0.07	0.08	0.45	0.09	0.46	0.98
4	1000	1550	0.23	0.11	0.02	0.13	0.45	0.06	0.48	0.98
5	1400	1550	0.46	0.00	0.12	0.00	0.42	0.00	0.43	0.98
6	50	300	0.00	0.00	0.63	0.37	0.00	0.00	0.55	0.91

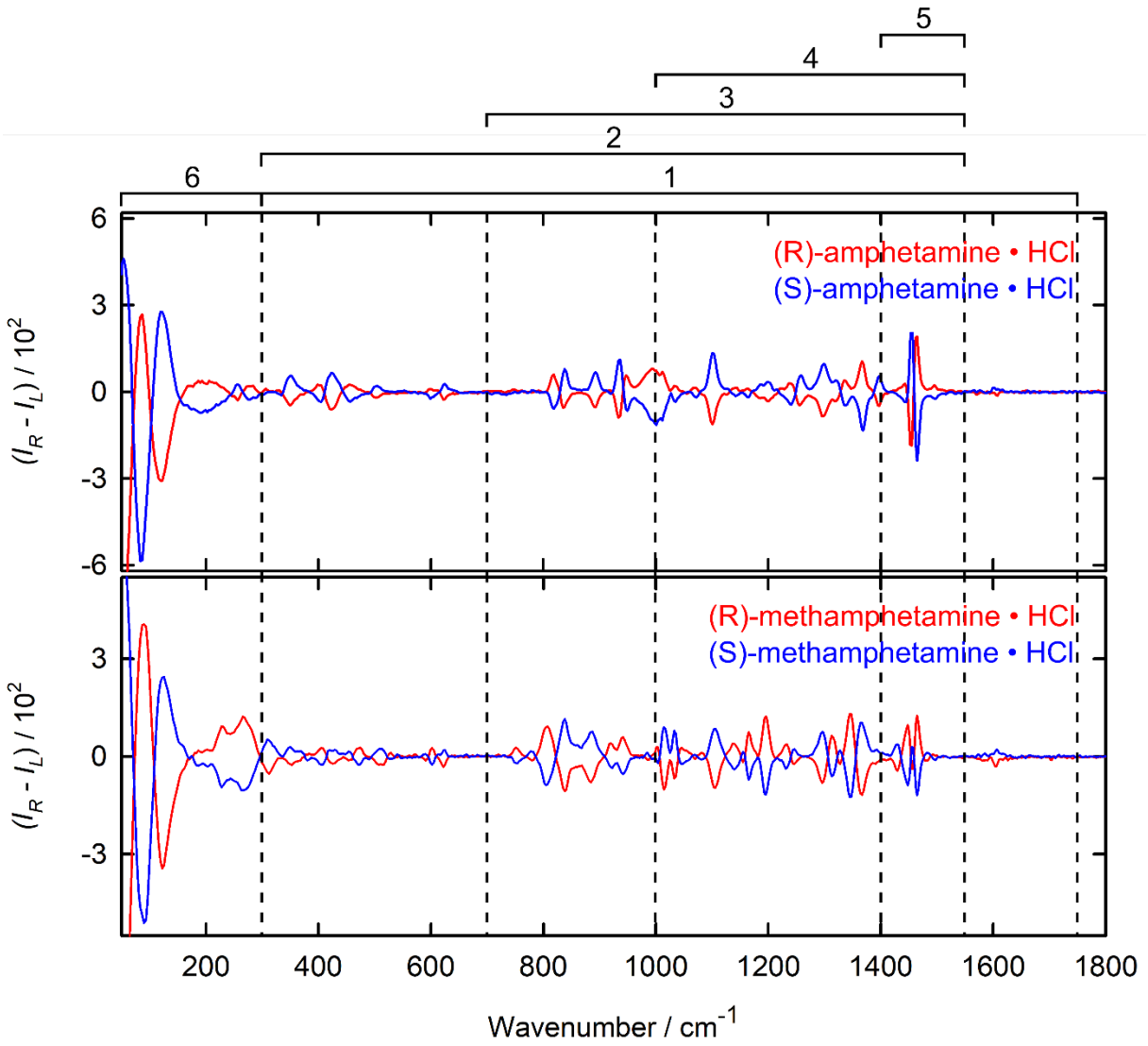

Fig. S16 Experimental ROA spectra of both amphetamine (top) and methamphetamine (bottom) hydrochloride enantiomers. Intervals **1 – 6** labels selected spectral ranges from **Table S9**.

The wavenumber scaling factor should be taken with caution. Similarity overlap can reach different maxima with the change of the scaling factor as can be observed for example for amphetamine similarity overlaps in **Fig. S17**. Most of the time, the best similarity overlap is unambiguously determined. However, a relatively large similarity can also be reached by the overlap with the similar spectral pattern adjacent to the analyzed spectral interval. For the cluster-based amphetamine model, the overlap with the VCD experiment is SimVCD = 0.27 and SimVCD = 0.73 for wavenumber factor of value 0.88 and 0.98, respectively. In the first case the large scaling factor leads to the wrong similarity overlap.

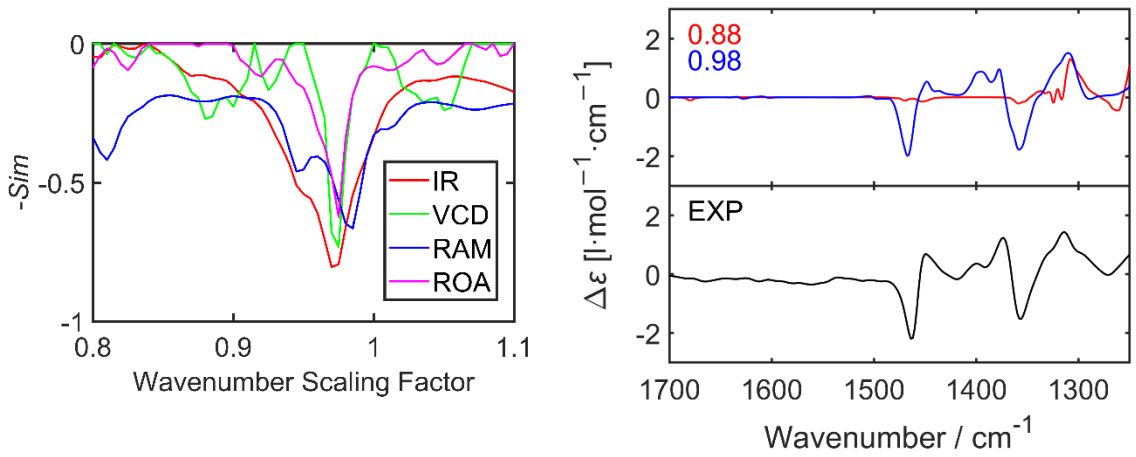

Fig. S17 Dependence of spectral similarity overlap on chosen wavenumber scaling factor for IR, VCD, Raman and ROA comparison of amphetamine experimental spectra and the cluster-based model (right). Example of VCD spectra overlaps for two different scaling factors (right).

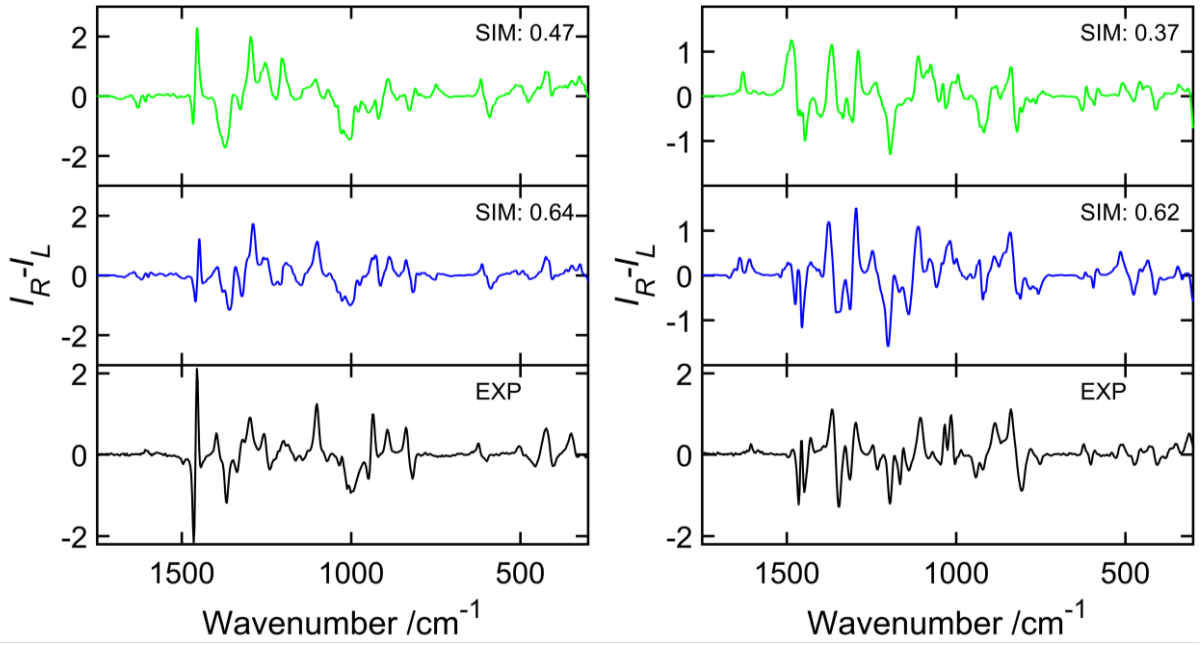

Fig. S18 Comparison of the (*S*)-amphetamine (left) and (*S*)-methamphetamine (right) ROA spectrum of the solute-solvent clusters weighted by the corresponding conformer populations from the MD distribution (green) and determined by the optimization algorithm (blue) to the experiment (black).

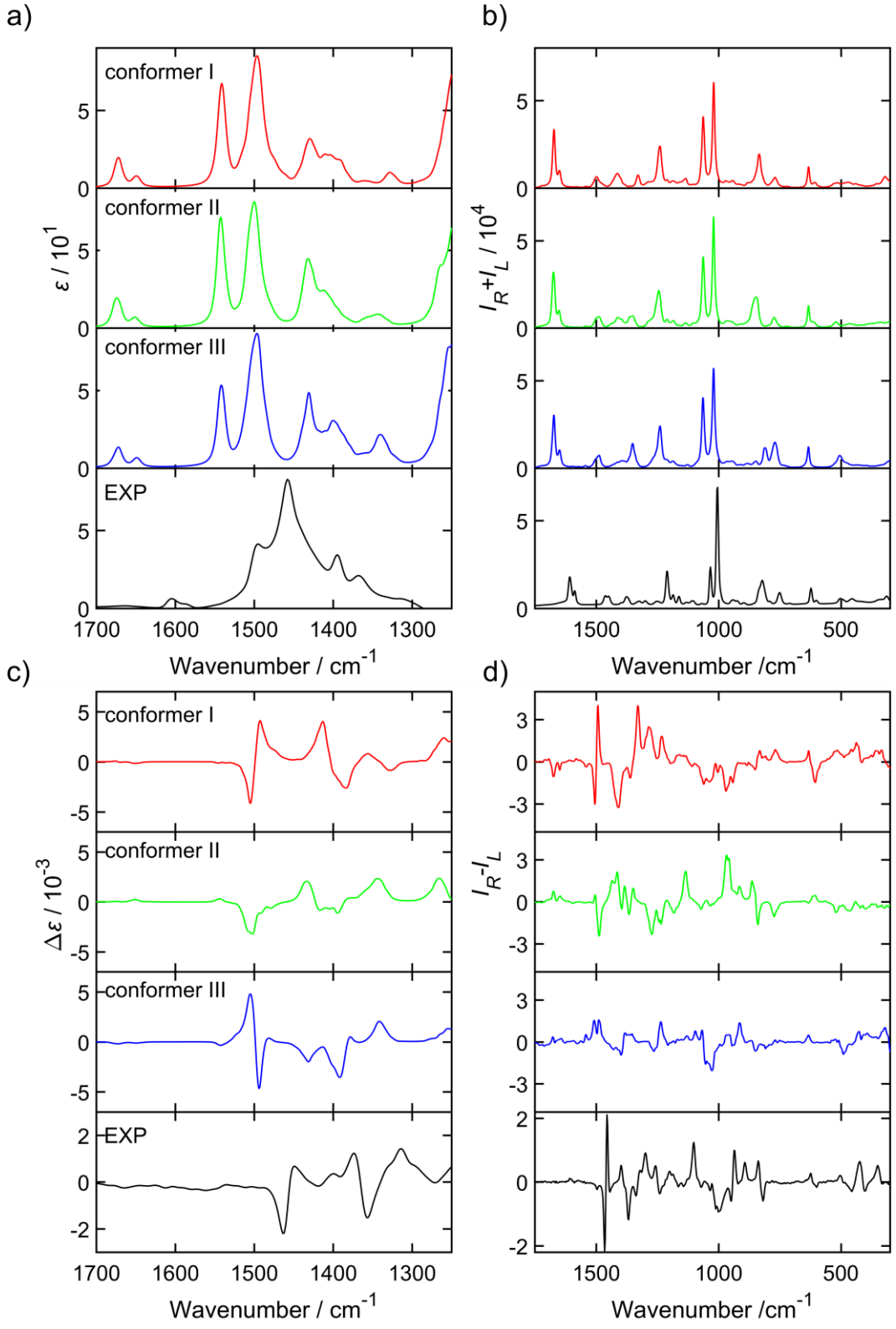

Fig. S19 IR (a), Raman (b), VCD (c) and ROA (d) spectra of the three amphetamine conformers (average of 100 snapshots per conformer, MD cluster-based model, 1st solvation shell) compared to the experiment.

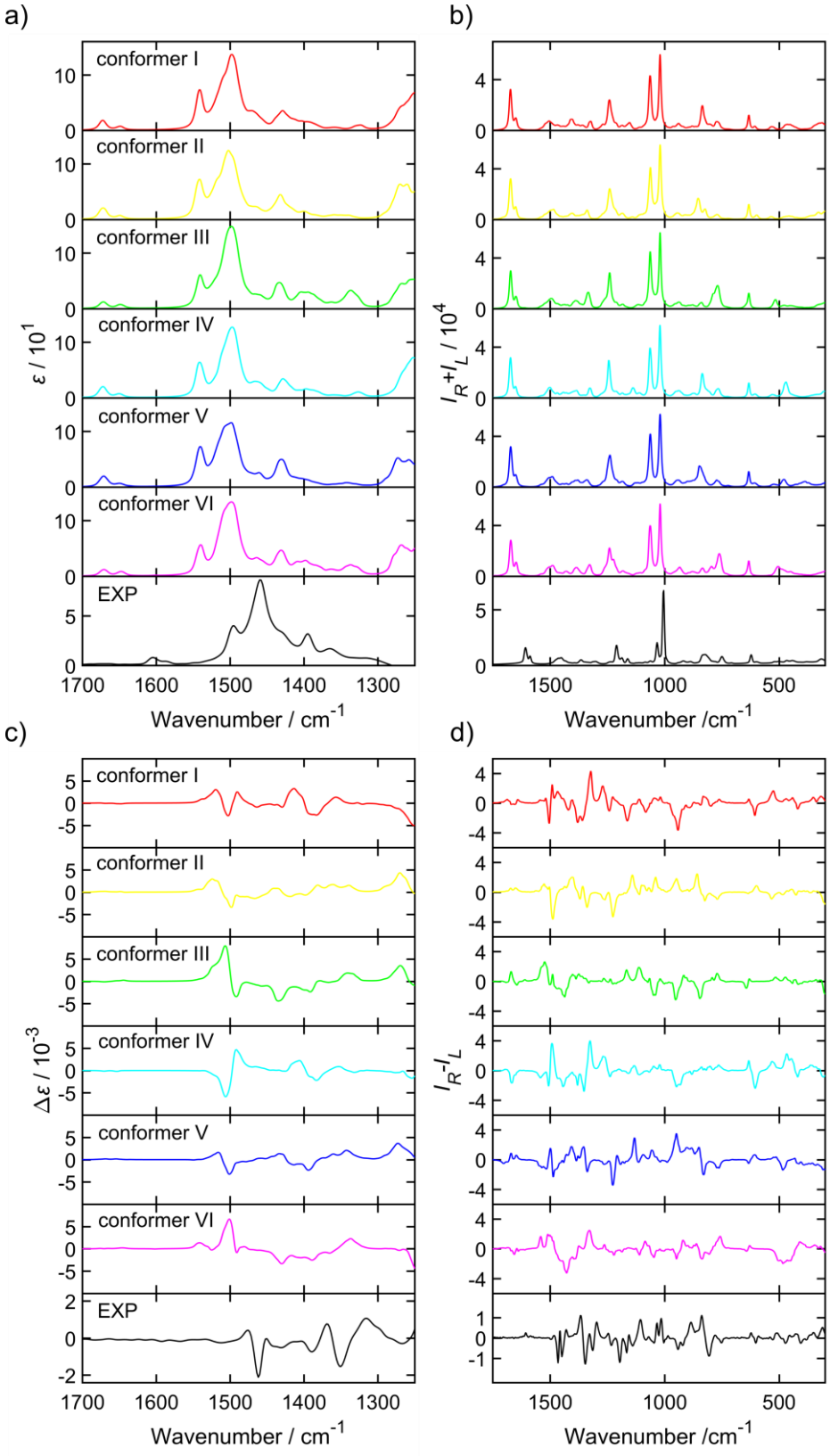

Fig. S20 IR (a), Raman (b), VCD (c) and ROA (d) spectra of the six methamphetamine conformers (average of 100 snapshots per conformer, MD cluster-based model, 1st solvation shell) compared to the experiment.

Table S10 Comparison of ROA similarity factors for linear combination of amphetamine three conformers. Predicted spectra based on the MD geometries with explicit water molecules (averaged 100 snapshots per conformer, B3PW91/rDPS/GD3BJ/COSMO, 300–1750 cm^{-1}) are compared to the experimental ROA spectra of (*R*)-amphetamine hydrochloride exported in five blocks of 2.58 hours of total accumulation time.

Exp. Block	Linear combination coefficients			Similarity Factor	Scaling Factor
	I	II	III		
1	0.45	0.42	0.14	0.63	0.9734
2	0.43	0.41	0.16	0.61	0.9736
3	0.44	0.41	0.15	0.62	0.9738
4	0.45	0.40	0.15	0.61	0.9736
5	0.44	0.40	0.16	0.60	0.9737
Std.dev =	0.01	0.01	0.01	0.01	0.0001

Table S11 Comparison of ROA similarity factors for linear combination of amphetamine three conformers. Predicted spectra based on the MD geometries with explicit water molecules (set of 5 spectra, averaged 20 snapshots per conformer, B3PW91/rDPS/GD3BJ/COSMO, 300–1750 cm^{-1}) are compared to the experimental ROA spectrum of amphetamine hydrochloride (enantiomer average "(*S*–*R*)/2").

Set	Linear combination coefficients			Similarity Factor	Scaling Factor
	I	II	III		
1	0.45	0.45	0.10	0.56	0.974
2	0.42	0.33	0.25	0.55	0.973
3	0.46	0.41	0.13	0.50	0.973
4	0.45	0.35	0.20	0.50	0.975
5	0.43	0.39	0.18	0.54	0.975
Std.dev =	0.02	0.05	0.06	0.03	0.001

Table S12 Comparison of ROA similarity factors for linear combination of amphetamine three conformers. Predicted spectra based on the MD geometries with explicit water molecules (cumulative averaged from 20 to 100 snapshots per conformer, B3PW91/rDPS/GD3BJ /COSMO, 300–1750 cm^{-1}) are compared to the experimental ROA spectrum of amphetamine hydrochloride (enantiomer average "(*S*−*R*)/2").

Number of snapshots	Linear combination coefficients			Similarity Factor	Scaling Factor
	I	II	III		
20	0.45	0.45	0.10	0.56	0.9737
40	0.43	0.39	0.17	0.62	0.9734
60	0.44	0.41	0.15	0.61	0.9732
80	0.43	0.40	0.17	0.61	0.9738
100	0.43	0.41	0.16	0.64	0.9740
Std.dev =	0.01	0.02	0.03	0.03	0.0003

Table S13 Comparison of ROA similarity factors for linear combination of methamphetamine conformers. Predicted spectra based on molecular dynamics (averaged 100 snapshots per conformer, B3PW91/rDPS/GD3BJ/COSMO, 300–1750 cm^{-1}) are compared to the experimental ROA spectrum of methamphetamine hydrochloride (enantiomer average "(*S*–*R*)/2"). Less populated methamphetamine conformers III, IV and VI are systematically excluded from the comparison.

Step	Linear combination coefficients						Similarity factor	Scaling Factor
	I	II	III	IV	V	VI		
1	0.37	0.29	0.05	0.00	0.26	0.03	0.63	0.98
2	0.37	0.29	0.05	XXX	0.26	0.03	0.63	0.98
3	0.38	0.28	0.06	XXX	0.28	XXX	0.62	0.98
4	0.40	0.31	XXX	XXX	0.28	XXX	0.62	0.98

Table S14 Linear combination coefficients of three stable conformers and similarity factor of amphetamine calculated for different MD cluster-based models including only one, two or three closest water molecules and the cluster with the whole first solvation shell.

MD model	Scaling Factor	Linear combination coefficients			Similarity factor
		I	II	III	
ROA (1750–300 cm^{-1})					
1 water	0.977	0.40	0.35	0.25	0.53
2 waters	0.976	0.40	0.36	0.24	0.63
3 waters	0.975	0.42	0.37	0.22	0.63
1^{st} shell	0.974	0.43	0.41	0.16	0.64
VCD (1700–1250 cm^{-1})					
1 water	0.974	0.43	0.45	0.12	0.79
2 waters	0.974	0.44	0.50	0.06	0.81
3 waters	0.974	0.44	0.51	0.05	0.81
1^{st} shell	0.973	0.40	0.47	0.13	0.82

Table S15 Linear combination coefficients of six stable conformers and similarity factor of methamphetamine calculated for different MD cluster-based models including only one, two or three closest water molecules and the cluster with the whole first solvation shell.

MD model	Scaling Factor	Linear combination coefficients						Similarity factor
		I	II	III	IV	V	VI	
ROA (1750–300 cm^{-1})								
1 water	0.982	0.32	0.37	0.06	0.00	0.22	0.03	0.51
2 waters	0.981	0.32	0.40	0.05	0.00	0.18	0.05	0.53
3 waters	0.980	0.34	0.32	0.07	0.00	0.24	0.04	0.57
1^{st} shell	0.976	0.37	0.29	0.05	0.00	0.26	0.03	0.63
VCD (1700–1250 cm^{-1})								
1 water	0.974	0.11	0.10	0.12	0.32	0.35	0.00	0.67
2 waters	0.974	0.11	0.15	0.14	0.32	0.27	0.00	0.67
3 waters	0.974	0.11	0.10	0.15	0.34	0.30	0.00	0.64
1^{st} shell	0.972	0.10	0.09	0.15	0.34	0.32	0.00	0.68